General Polynomial Factorization-Based Design of Sparse Periodic Linear Arrays

Sanjit K. Mitra, *Life Fellow, IEEE*, Kalyan Mondal, *Senior Member, IEEE*, Mikhail K. Tchobanou, *Member, IEEE*, and Gordana Jovanovic Dolecek, *Senior Member, IEEE*

***Abstract*—We have developed several methods of designing sparse periodic arrays based upon the polynomial factorization method. In these methods, transmit and receive aperture polynomials are selected such that their product results in a polynomial representing the desired combined transmit/receive (T/R) effective aperture function. A desired combined T/R effective aperture is simply an aperture with an appropriate width exhibiting a spectrum that corresponds to the desired two-way radiation pattern. At least one of the two aperture functions that constitute the combined T/R effective aperture function will be a sparse polynomial. A measure of sparsity of the designed array is defined in terms of the element reduction factor. We show that elements of a linear array can be reduced with varying degrees of beam mainlobe width to sidelobe reduction properties.**

I. Introduction

The design of linear phased arrays has been of interest for many years with applications in imaging systems using ultrasound, radar, sonar, and seismic signals [1]–[3]. For example, such arrays are used to electronically steer or focus the received signals to enhance ultrasound image resolution. The number of elements, their weights, and element spacing in the array generally determine the level of control over the ultrasound beam. The cost of a scanner, especially for 2-D imaging, can be reduced by using sparse arrays with multiple missing elements. However, periodic sparse arrays obtained either algorithmically or by using heuristic optimization techniques can result in unwanted grating lobes in the radiation pattern. One way to avoid such a grating lobe in a periodic array is to use a two-way radiation pattern generated by a pair of transmit and receive arrays with proper periodicities and different spacings [4]. The convolution of these arrays can result in a full array or a near-full array with minimum mainlobe width, high sidelobe rejection, and control over unwanted grating lobes.

Manuscript received September 7, 2009; accepted May 9, 2010. This work was supported in part by a University of California MICRO grant with matching supports from the Intel Corp., Microsoft Corp. and Xerox Corp., and a Fairleigh Dickinson University Research Grant-in-Aid.

S. K. Mitra is with the Ming Hsieh Department of Electrical Engineering, University of Southern California, Los Angeles, CA.

K. Mondal is with the Gildart Haase School of Computer Sciences and Engineering, Fairleigh Dickinson University, Teaneck, NJ (e-mail: mondal@fdu.edu).

M. K. Tchobanou is with the Department of Electrical Physics, Moscow Power Engineering Institute Technical University, Moscow, Russia.

G. Jovanovic-Dolecek is with the Electronics Department, Instituto Nacional de Astrofísica, Óptica y Electrónica, Puebla, Mexico.

Digital Object Identifier 10.1109/TUFFC.2010.1643

An objective of sparse array design is to enhance image resolution, which is achieved through minimizing the peak sidelobe height and mainlobe width. Additionally, focused beamforming for elimination of interference signals is another major goal. Many well-known researchers have formulated algorithms for optimized array design. Steinberg [1], [5] introduced design of thinned arrays with randomly located elements to reduce peak sidelobe and compared it with existing algorithmic techniques. Linear programming based algorithms have been used by [6] and [7] for reduced sidelobe thinned array design. Haupt and others [8]–[13] showed how to optimally thin large arrays using genetic algorithms (GA). Simulated annealing-based techniques to synthesize the position and weight coefficients of a linear array that minimizes peak sidelobes were proposed by Trucco, *et al.* [14], [15]. Austeng, *et al.* [16] proposed the design of 2-D radially sparse periodic and non-overlapping layouts with the possibility of trading off between sidelobe peaks and sidelobe energy. Caorsi, *et al.* [12] applied a customized GA to adaptively eliminate interfering signals in 3-D scanner design. Recently a hybrid approach [17] combining particle swarm optimization (PSO) with combinatorial techniques has been proposed for the synthesis of planar thinned arrays.

Lockwood, *et al.* [4] proposed multiple algorithmic strategies for designing sparse periodic arrays using the combined transmit/receive (T/R) effective aperture function. The strategies proposed (except for synthetic aperture) are somewhat intuitive and it is not obvious how to extend them to any arbitrary array size. Their proposed vernier interpolation technique has been used in commercial scanner designs with a 31–element sparse array and was extended to 2-D array designs [8]. Although vernier interpolation leads to excellent image resolution, other techniques such as staircase effective aperture function obtained through rectangular interpolation [18]–[22] can also lead to good designs.

In a manner analogous to window-based finite impulse response (FIR) filter design [18], a sparse array based combined T/R effective aperture function can be chosen based upon the requirements on sidelobe rejection and mainlobe width. Further optimization of the beampattern can be undertaken using optimization techniques proposed in several papers including [10]. Minimization of the number of transducers beyond optimization of sparse array sizes also needs to be addressed to reduce the cost of high-speed imaging systems.

Limiting the number of elements in 1-D arrays has not been a major issue for ultrasound imaging for about a decade. With new transducer technologies and software beamformers working on general purpose processors, sparse 1-D arrays are not of great interest. However, this is not the case for 2-D arrays [16], [17]. Large, fully sampled 2-D arrays still require electronic channel counts beyond the current state of the art. Approximation methods are used in current clinical systems, hence, a robust approach to creating sparse arrays may still be interesting for clinical applications. Because 2-D arrays can be formed out of 1-D arrays, assuming the 2-D array to be separable, simple design of robust 1-D array as postulated in this paper will be of interest to the ultrasound imaging practitioners.

The main contributions from this paper are as follows. After introducing the mathematical notations in Section II, we describe a general polynomial factorization scheme [19] in Section III and apply it to the design of different periodic linear sparse arrays. Sections IV through VII include the designs of uniform, linearly tapered, staircase, and mixed tapered staircase arrays proposed in [19]–[22] under a common framework with specific design steps and illustrative examples. Our polynomial factorization-based mathematical framework is extended to the previously proposed [4] triangular and vernier interpolation schemes. Some properties of triangular and vernier interpolations became obvious from this formulation and are described under Sections VIII and IX. In Section X, we compare all of the sparse arrays designed in the examples as well as those for a combined T/R effective 85-element-long full array. The comparison table could be used as a guideline to choosing one or more design techniques to be used for the specific image scanner or antenna beamformer design.

II. Mathematical Notations

The far-field radiation pattern at an angle θ away from the broadside of a linear array [2] with N isotropic, equispaced elements is given by

$$P(u) = \sum_{n=0}^{N-1} w_{\mathrm{eff}}(n) e^{j[2\pi(u/\lambda)d]n}, \tag{1}$$

where the aperture function $w_{\mathrm{eff}}(n)$ is the element weighting function which depends on the element position n, λ is the wavelength, $u = \sin\theta$, and d is the inter-element spacing. We consider here the case of a two-way radiation pattern generated by a pair of transmit and receive arrays. In this case, the design reduces to the design of a combined T/R effective aperture function $w_{\mathrm{eff}}(n)$ given by the convolution of the transmit and receive aperture functions, $w_{\mathrm{T}}(n)$ and $w_{\mathrm{R}}(n)$, respectively [4]:

$$w_{\mathrm{eff}}(n) = w_{\mathrm{T}}(n) * w_{\mathrm{R}}(n). \tag{2}$$

The number of elements N in a single array with a combined T/R effective aperture function $w_{\mathrm{eff}}(n)$ is given by $N = T + R - 1$, where T is the number of elements (including the missing elements) in the transmit array $w_{\mathrm{T}}(n)$ and R is the number of elements (including the missing elements) in the receive array $w_{\mathrm{R}}(n)$.

By substituting

$$x = e^{j2\pi ud/\lambda}, \tag{3}$$

the combined T/R effective, transmit, and receive aperture functions can be expressed as polynomials:

$$P_{\mathrm{eff}}(x) = \sum_{n=0}^{N-1} w_{\mathrm{eff}}(n) x^n, \tag{4}$$

$$P_{\mathrm{T}}(x) = \sum_{n=0}^{T-1} w_{\mathrm{T}}(n) x^n, \tag{5}$$

$$P_{\mathrm{R}}(x) = \sum_{n=0}^{R-1} w_{\mathrm{R}}(n) x^n. \tag{6}$$

It follows that (2) can be rewritten in the form

$$P_{\mathrm{eff}}(x) = P_{\mathrm{T}}(x) P_{\mathrm{R}}(x). \tag{7}$$

It has been shown that in such cases, it is possible to use sparse transmit and receive arrays with a combined T/R effective aperture function that is a close equivalent to that of a single array with no missing elements [4], [18]–[22], i.e., a full array.

In this paper, we outline methods of designing sparse transmit and receive arrays based on the factorization of polynomial $P_{\mathrm{eff}}(x)$ as a product of two lower order polynomials, $P_{\mathrm{T}}(x)$ and $P_{\mathrm{R}}(x)$, with some zero-valued coefficients. Each of the methods described herein results in arrays with different layouts of varying properties; one could either use the designed arrays as is or use them as a starting point for further optimization.

III. A General Factorization Method

Our sparse array design methods are based on the factorization of a polynomial $P_M(x)$ of degree M in positive powers of x and with unity coefficients [18], [19]:

$$P_M(x) = \sum_{i=0}^{M} x^i. \tag{8}$$

The number of coefficients in $P_M(x)$ is given by $M + 1$.

Theorem [19]: Let the positive integer $M + 1$ be expressible as a product of $K + 1$ irreducible positive integers $M_k + 1$, $0 \le k \le K$, i.e.,

$$M + 1 = \prod_{k=0}^{K} (M_k + 1). \tag{9}$$

Then $P_M(x)$ can be expressed in the form

$$P_M(x) = \prod_{k=0}^{K} P_{M_k}(x^{S_k}), \tag{10}$$

where

$$S_k = \prod_{j=0}^{k} (M_{j-1} + 1), \;\; M_{-1} = 0, \tag{11}$$

Proof: The proof of the decomposition in (10) is by induction and is included in [19].

The factorization of a specified composite number $M + 1$ into a product of irreducible integers can be carried out using Euclid's algorithm. A special case is when $M + 1$ can be expressed as a power of two, namely

$$M + 1 = 2^{\nu}, \tag{12}$$

where ν is an integer. Then the factorization in (10) reduces to

$$P_M(x) = (1 + x)(1 + x^2)\cdots(1 + x^{2^{\nu-1}}). \tag{13}$$

The decomposition in (13) has been used in designing sparse antenna arrays with a uniform aperture function and a linearly tapered aperture function [18].

IV. Sparse Array Design With Uniform Effective Aperture Function

The design steps based upon discussions of the previous sections are outlined here.

1) Determine or choose the order M of the combined T/R effective aperture function $P_{\text{eff}}(x)$. Compute the parameters sidelobe rejection (SR) and mainlobe width (MW), defined in Section X, to make sure that choice of $M + 1$ meets the design specifications.
2) Factorize $M + 1$ into $K + 1$ prime integers $M_0 + 1, M_1 + 1, \ldots, M_K + 1$ using (9). It is obvious that no further design steps can be taken if $M + 1$ is a prime number.
3) Factorize $P_{\text{eff}}(x)$ into $K + 1$ prime factors as in (10).
4) Associate K_{T} prime factors with $P_{\text{T}}(x)$ so that the smaller aperture is for the transmit array and the remaining $K + 1 - K_{\text{T}}$ factors are with $P_{\text{R}}(x)$.
5) Compute the sparsity factor (SF) parameter, defined in Section X, to determine acceptability of the design. If it is not acceptable, go back to step 4 to find another sparse solution.

Example 1:

Consider $M = 17$, i.e., $P_{17}(x) = \sum_{i=0}^{17} x^i$. In this case, $K = 2$ and one factorization is given by

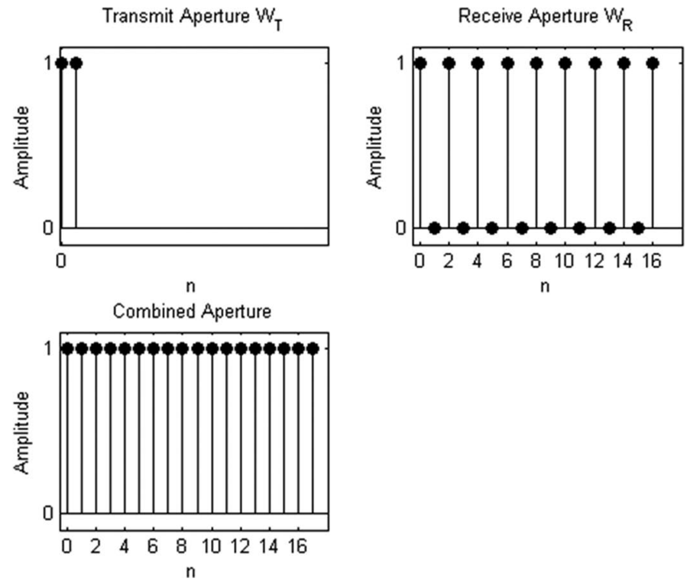

Fig. 1. Design #1 of Example 1.

$$P_{17}(x) = (1 + x)(1 + x^2 + x^4)(1 + x^6 + x^{12}).$$

There are three possible practical array designs resulting from this factorization.

Design #1: We can choose

$$\begin{aligned} P_{\text{T}}(x) &= 1 + x, \\ P_{\text{R}}(x) &= (1 + x^2 + x^4)(1 + x^6 + x^{12}) \\ &= 1 + x^2 + x^4 + x^6 + x^8 + x^{10} + x^{12} + x^{14} + x^{16}. \end{aligned}$$

This design uses 11 antenna elements, 2 in the transmit array and 9 in the receive array, resulting in an SF of $18/11 = 1.636$. Both receive and transmit arrays are periodic, which is characteristic of the uniform effective aperture function. The transmit array elements are $\lambda/2$ apart, whereas those of the receive array are λ apart. The array patterns are shown in Fig. 1.

Design #2: Now we choose

$$\begin{aligned} P_{\text{R}}(x) &= 1 + x^6 + x^{12}, \\ P_{\text{T}}(x) &= (1 + x)(1 + x^2 + x^4) \\ &= 1 + x + x^2 + x^3 + x^4 + x^5. \end{aligned}$$

The total number of antenna elements needed for this design is 9, leading to an SF of $18/9 = 2$. The SF for this design is better than that obtained in Design #1. In this case, receive and transmit array elements are respectively 3λ and $\lambda/2$ apart. The array patterns are shown in Fig. 2.

Design #3: A third design with 9 elements is also possible. The arrays are shown in Fig. 3. This exhibits a different spacing pattern of array elements compared with

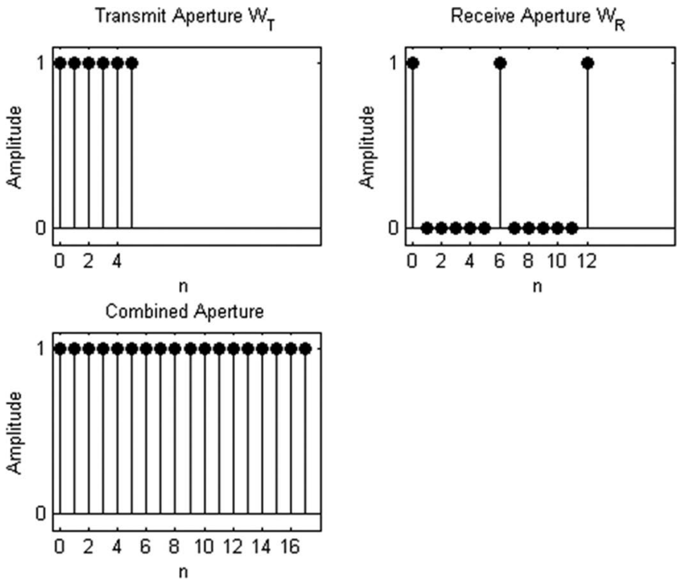

Fig. 2. Design #2 of Example 1.

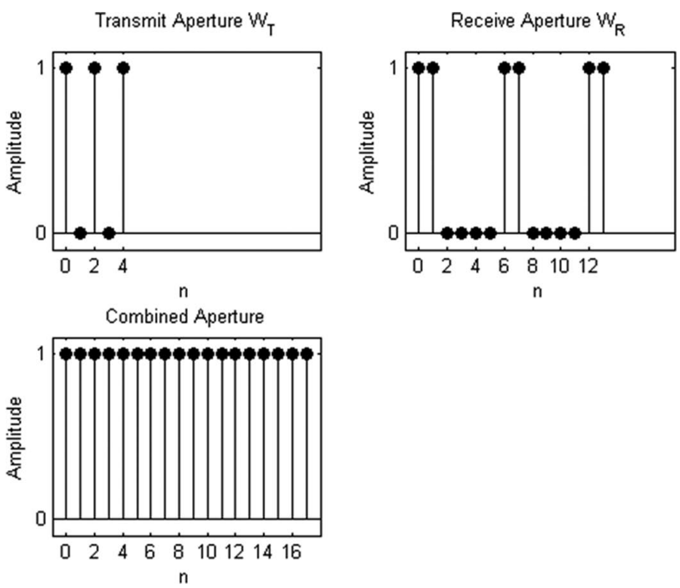

Fig. 3. Design #3 of Example 1.

that shown in Figs. 1 and 2. Here, the receive array does not exhibit a uniform spacing although the transmit array elements are λ apart.

Example 2:

In this example, we again choose $K = 2$ and

$$P_{26}(x) = \sum\nolimits_{i=0}^{26} x^i = (1 + x + x^2)(1 + x^3 + x^6)(1 + x^9 + x^{18}).$$

Again, there are three different designs possible and all of them require 12 antenna elements, giving an SF of 27/12 = 2.25. For the design given,

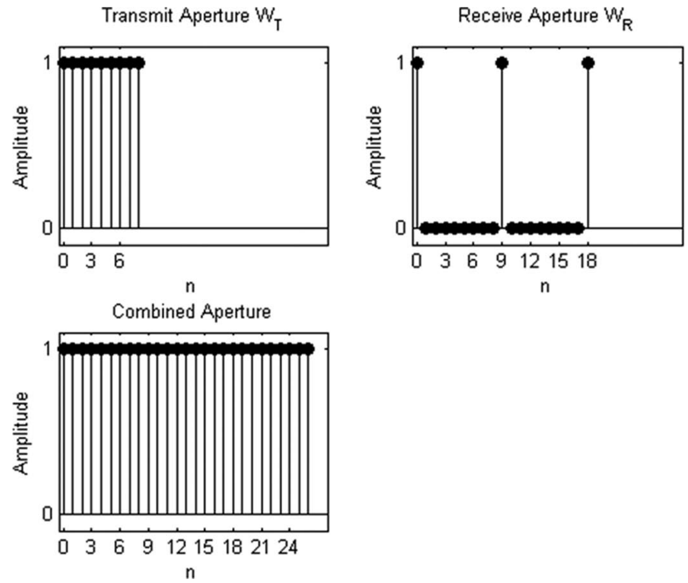

Fig. 4. Transmit, receive, and combined T/R apertures for Example 2.

$$P_{\mathrm{T}}(x) = \sum_{i=0}^{8} x^i, \quad P_{\mathrm{R}}(x) = \sum_{i=0}^{2} x^{9i},$$

the pattern of the combined T/R effective aperture function and the corresponding transmit and receive apertures are shown in Fig. 4. Clearly, the transmit array elements are $\lambda/2$ apart, whereas the receive elements are $9\lambda/2$ apart.

It should be noted from Examples 1 and 2 that an increase in M (from 17 to 26) improves the MW (from 0.0938 to 0.0625) of the design without affecting the SR of −13.2 dB. This is due to the property of the uniform effective aperture function. The design in Example 2 with a larger M also exhibits a better SF.

V. Sparse Array Design With Linearly Tapered Effective Aperture Function

For the design of a sparse array pair with a linearly tapered effective aperture function $P_{\mathrm{eff}}(x)$, we choose

$$P_{\mathrm{eff}}(x) = P_r(x)P_s(x), \tag{14}$$

where

$$P_r(x) = \frac{1}{r}\sum_{i=0}^{r-1} x^i, \quad P_s(x) = \sum_{i=0}^{s-1} x^i. \tag{15}$$

The number of elements in the combined T/R effective aperture function is then

$$N = r + s - 1. \tag{16}$$

The parameter s must satisfy the condition

$$s > r - 1. \tag{17}$$

TABLE I. Summary of Results From Design Examples in This Paper.

Example	Type	N_T	N_R	N_{eff}	SF	ERF	Leakage factor (%)	Mainlobe width (rad)	Sidelobe rejection (dB)	SNR loss (dB)	Composite SNR loss (dB)
1 #1	Uniform	2	9	18	1.64		9.53	0.0977	−13.2	0	2.7621
1 #2	Uniform	6	3	18	2.00		9.53	0.0977	−13.2	0	6.3682
1 #3	Uniform	3	6	18	2.00		9.53	0.0977	−13.2	0	8.1167
2	Uniform	9	3	27	2.25		9.54	0.0645	−13.2	0	8.0163
3	Linearly tapered	20	30	85	1.70	1.72	0.14	0.0273	−31.8	1.1137	3.4242
4	Staircase	16	18	60	1.76	1.2	1.41	0.0371	−21	0.826	6.6511
5	Staircase	18	17	81	2.31	1.63	0.58	0.0273	−30.9	0.8811	9.8623
5	Staircase with apodization	18	17	81	2.31	1.63	0.14	0.0332	−36.7	1.5727	9.8623
6	Mixed tapered staircase	25	68	144	1.55	1.13	0.26	0.0166	−31.3	1.1194	7.8395
6	Mixed tapered staircase with apodization	25	68	144	1.55	1.13	0.05	0.0186	−35.3	1.6611	7.8395
7	Triangular	7	5	23	1.92		0.34	0.1055	−26.1	1.0796	5.3148
8	Triangular	21	19	119	2.98		0.28	0.0195	−26.5	1.2136	12.8433
9	Vernier ($p = 3$)	15	22	85	2.30	2.24	1.00	0.0273	−26.4	1.0882	12.058
9	Vernier with apodization	15	22	85	2.30	2.24	0.39	0.0313	−32.4	1.4995	12.058
10	Vernier ($p = 4$)	22	17	128	3.28	3.13	1.68	0.0176	−26.4	1.1192	14.8957

The design steps are as follows.

1) Determine or choose the order N of the combined T/R effective aperture function $P_{\text{eff}}(x)$. Compute the parameters SR and MW to make sure that the choice of N meets the design specifications.
2) Divide N into two components r and s satisfying (16) and (17) and making sure that at least one of these components is a composite number like $M + 1$ that can be factorized using (9).
3) Select $P_r(x)$ and $P_s(x)$ using (15).
4) Factorize $P_r(x)$ and/or $P_s(x)$ into factors as in (10).
5) Associate some factors from $P_r(x)$ and $P_s(x)$ with $P_T(x)$ and the rest of the factors with $P_R(x)$ so that the transmit array has a smaller aperture than the receive array.
6) Compute the SF parameter to determine acceptability of the design. If it is not acceptable, go back to step 5 to find another sparse solution.

Example 3:

As an example of designing a linearly tapered array, we choose $r = 36$, $s = 50$.

Thus

$$P_r(x) = \frac{1}{36}\sum_{i=0}^{35} x^i = (1+x)(1+x^2)(1+x^4+x^8)(1+x^{12}+x^{24}),$$

$$P_s(x) = \sum_{i=0}^{49} x^i = (1+x)(1+x^2+x^4+x^6+x^8) \times (1+x^{10}+x^{20}+x^{30}+x^{40}).$$

The SR has improved to −31 dB as seen from Table I.

The transmit and receive arrays could also be chosen as

$$P_T(x) = (1+x)(1+x^2)(1+x^4+x^8) \times (1+x^2+x^4+x^6+x^8),$$

$$P_R(x) = \frac{1}{36}(1+x)(1+x^{12}+x^{24}) \times (1+x^{10}+x^{20}+x^{30}+x^{40}).$$

Plots of the corresponding transmit and receive array patterns are shown in Fig. 5. In this case, the element reduction factor (ERF, defined in Section X) is $(36 + 50)/(30 + 20) = 1.72$. The transmit array is periodic with elements spaced $\lambda/2$ apart, but the receive array is not equally spaced.

VI. Sparse Array Design With Staircase Effective Aperture Function

For the design of an array pair with a staircase effective aperture function, there are three possible cases described in this section.

A. Even Number of Unequal Step Sizes

In this case, the factor $P_r(x)$ is of the form

$$P_r(x) = \frac{1}{2\ell+1}[1 + x^{k_1}(1 + x^{k_2}(1 + \cdots + x^{k_\ell}(1 + \cdots + x^{k_2}(1 + x^{k_1})\cdots))))]. \quad (18)$$

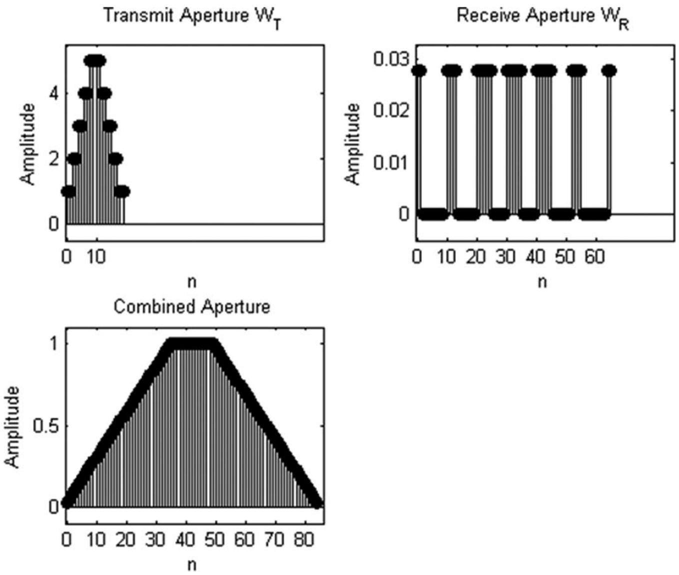

Fig. 5. Linearly tapered array design of Example 3.

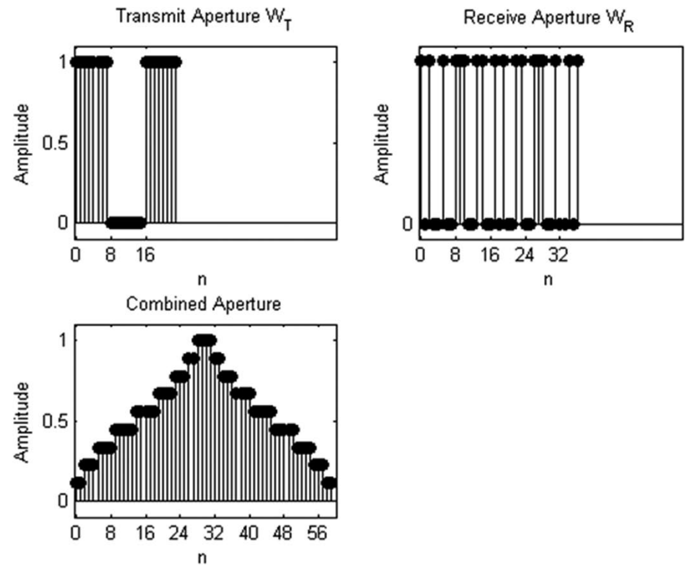

Fig. 6. Staircase array design for Example 4.

The number r of elements (including zero-valued ones) in $P_r(x)$ is given by

$$r = 2\sum_{i=1}^{\ell} k_i + 1. \tag{19}$$

Note that different choices for integer values of k_i can lead to different designs. A proper choice of k_i can lead to optimizing either the MW or the SR.

Because $P_r(x)$ may already be sparse by choice, we use ERF for staircase-like combined T/R effective aperture function designs. The ERF and SF are identical in the cases of uniform and linear tapered effective aperture functions.

An example design of sparse arrays with a staircase effective aperture function for $\ell = 2$ is included in [21, Example 3]. We present another, more complex, design example to introduce ERF (in comparison with SF) as a figure of merit.

Example 4: Let $k_1 = 2$, $k_2 = 3$, $k_3 = 4$, $k_4 = 5$, $\ell = 4$, and $s = 32$. Here

$$\begin{aligned} P_r(x) &= \frac{1}{9}[1 + x^2(1 + x^3(1 + x^4(1 + x^5(1 + x^5(1 + x^4(1 \\ &\quad + x^3(1 + x^2)))))))] \\ &= \frac{1}{9}(1 + x^2 + x^5 + x^9 + x^{14} + x^{19} + x^{23} + x^{26} + x^{28}), \end{aligned}$$

and

$$P_s(x) = \sum_{i=0}^{31} x^i = (1 + x)(1 + x^2)(1 + x^4)(1 + x^8)(1 + x^{16}).$$

The SR obtained in this case is -21 dB which is worse than the design in [21] by almost 3 dB, although the current design uses more full array elements (60 versus 26).

One possible efficient factorization of $P_{\text{eff}}(x)$ is given by

$$\begin{aligned} P_{\text{R}}(x) &= \frac{1}{9}(1 + x^2 + x^5 + x^9 + x^{14} + x^{19} + x^{23} + x^{26} + x^{28}) \\ &\quad \times (1 + x^8), \\ P_{\text{T}}(x) &= (1 + x + x^2 + x^3 + x^4 + x^5 + x^6 + x^7)(1 + x^{16}). \end{aligned}$$

A plot of the transmit, receive, and combined T/R designed arrays is shown in Fig. 6. Here the ERF is given by $(9 + 32)/(18 + 16) = 1.2$ although the SF is $60/34 = 1.8$.

Obviously, neither receive nor the transmit array exhibit equal spacing in this example.

B. Odd Number of Unequal Step Sizes

In this case, the factor $P_r(x)$ is of the form

$$\begin{aligned} P_r(x) = \frac{1}{2\ell}[1 + x^{k_1}(1 + x^{k_2}(1 + \cdots + x^{k_\ell}(1 + \cdots \\ + x^{k_2}(1 + x^{k_1})\cdots))))]. \end{aligned} \tag{20}$$

The number r of elements (including zero-valued ones) in $P_r(x)$ is given by

$$r = 2\sum_{i=1}^{\ell-1} k_i + k_\ell + 1. \tag{21}$$

For a staircase effective aperture function $P_{\text{eff}}(x)$, the number s of elements in $P_s(x)$ of (15) must satisfy the condition in (17).

An example design of sparse arrays with a staircase effective aperture function using an odd number of unequal step sizes is included as [21, Example 4].

C. Equal Step Sizes

In this case, the factor $P_r(x)$ is of the form

$$P_r(x) = \frac{1}{\ell + 1}[1 + x^{k_1}(1 + x^{k_2}(1 + \cdots + x^{k_{\ell-1}}(1 + x^{k_\ell})\cdots))]. \tag{22}$$

The number r of elements (including zero-valued ones) in $P_r(x)$ is given by

$$r = \ell k + 1. \tag{23}$$

The number of elements in the combined T/R effective aperture function in this case is then $N = \ell k + s$.

We illustrate the design of sparse arrays with a staircase effective aperture function for equal k_r values in the following example.

Example 5: Let $k_r = 6$, and $r = 1, \ldots, 5$. Then $P_r(x) = 1/6(1 + x^6 + x^{12} + x^{18} + x^{24} + x^{30})$ and $P_s(x) = \sum_{i=0}^{50} x^i$, which corresponds to $s = 51$. One possible efficient factorization of $P_{\text{eff}}(x)$ is given in [21] to be

$$P_{\mathrm{R}}(x) = \frac{1}{6}\sum\nolimits_{i=0}^{16} x^{3i}$$
$$P_{\mathrm{T}}(x) = (1 + x + x^2)(1 + x^6 + x^{12} + x^{18} + x^{24} + x^{30}).$$

The shape of the combined T/R effective aperture function, being a staircase, is considered somewhat ragged as seen in Fig. 7(a). Note that Fig. 7(b) shows the beamforming gain for an equivalent 79-element full array normalized to 0 dB, and the relative gain of the designed array with its combined T/R effective aperture function as shown in Fig. 7(a). The designed overall staircase array exhibits a different beam pattern and an SNR loss (as defined in Section X) of 0.8811 dB compared with the full array.

A cosine² apodization function can be applied as proposed in [4] which smoothes the overall aperture function. This requires application of cosine apodization on both receive and transmit apertures. Apodization increases the complexity of the feed network, if applied to the transmit aperture, and consequently there will be some energy loss compared with the uniform excitation distribution. Application of apodization on the receive aperture avoids this issue. As such, we will only apply cosine apodization on the receive aperture in the rest of the paper. An example weighting function for the even-order (N_{R} even) polynomial $P_{\mathrm{R}}(x)$ leading to a cosine apodization is noted here:

$$w_{\mathrm{R}}(i) = 0.15 + 0.85\cos[\pi(2i - N_{\mathrm{R}})/2N_{\mathrm{R}}]. \tag{24}$$

For such apodization, the resultant plot for this example is shown in Fig. 8. The SR has increased to -36.7 dB with no change in the SF. After apodization, all the receive element values are, in general, non-integer quantities. Thus, the signals from different receive antennas need to be weighted by the computed weight factors before addition to develop the desired combined T/R effective aperture function.

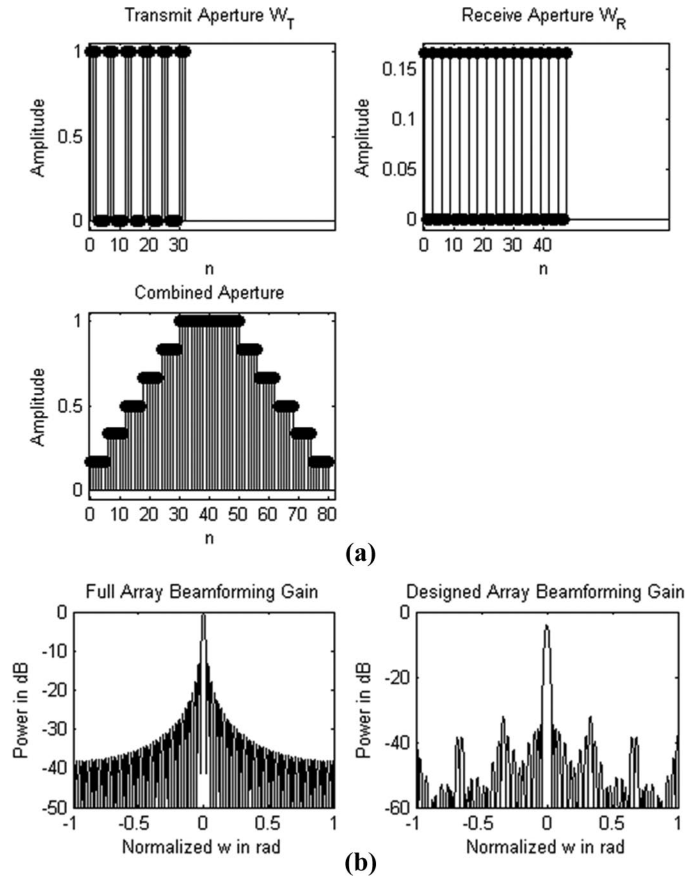

Fig. 7. (a) Staircase array design for Example 5 without apodization showing transmit, receive, and combined T/R apertures. (b) Staircase array design for Example 5 showing full array versus designed array beamforming gains.

VII. Sparse Array Design With Mixed Tapered Staircase Effective Aperture Function

In this case, the factor $P_r(x)$ is of the form

$$P_r(x) = \frac{1}{n(\ell + 1)} \times [P_3(x) + x^{k_1}(P_3(x) + x^{k_2}(P_3(x) + \cdots + x^{k_\ell}(P_3(x))\cdots))], \quad k_1 = k_2 = \cdots = k_\ell = k, \tag{25}$$

where

$$P_3(x) = 1 + \sum_{i=1}^{m} a_i x^i, \tag{26}$$

whose coefficients a_i are chosen properly to have a value of either 0 or 1 so that a staircase type aperture function can be guaranteed along with a reduction in array elements. Here $m < k$ and n is the number of nonzero terms in $P_3(x)$. The number of elements in the combined T/R effective aperture function is then $N = \ell k + m + s$.

We illustrate the design of sparse arrays with mixed tapered staircase effective aperture function for equal k_r values in the following example.

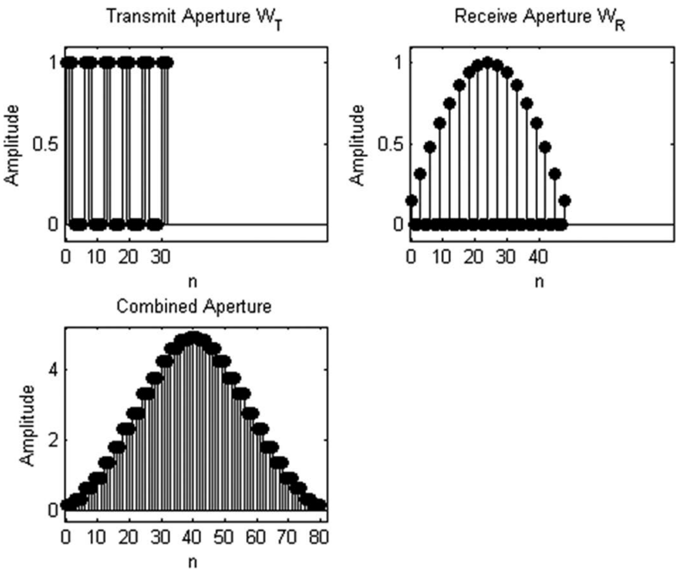

Fig. 8. Staircase array design for Example 5 with a cosine apodization applied to receive aperture.

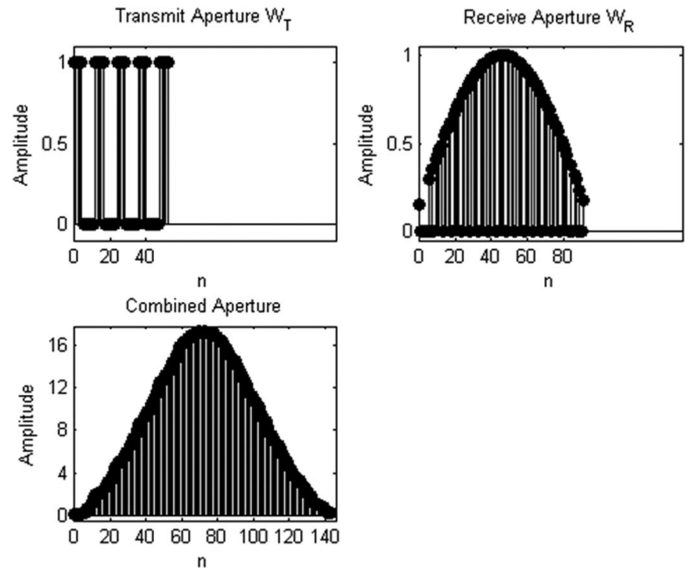

Fig. 9. Transmit, receive, and combined T/R effective apertures for Example 6 with an additional cosine apodization.

Example 6: Consider

$$k_1 = k_2 = k_3 = k_4 = 12, P_3(x) = 1 + x^7 + x^9 + x^{11}, \\ r = 60 \text{ and } s = 85.$$

The relevant polynomials are:

$$P_r(x) = \frac{1}{20}(1 + x^{12} + x^{24} + x^{36} + x^{48})(1 + x^7 + x^9 + x^{11})$$
$$P_s(x) = \sum_{i=0}^{84} x^i = (1 + x + x^2 + x^3 + x^4)\sum_{i=0}^{16} x^{5i}.$$

For example, these choices lead to transmit and receive sparse arrays as in [22]:

$$\begin{aligned} P_{\mathrm{T}}(x) &= (1 + x + x^2 + x^3 + x^4)(1 + x^{12} + x^{24} + x^{36} + x^{48}) \\ &= 1 + x + x^2 + x^3 + x^4 + x^{12} + x^{13} + x^{14} + x^{15} \\ &\quad + x^{16} + x^{24} + x^{25} + x^{26} + x^{27} + x^{28} + x^{36} + x^{37} \\ &\quad + x^{38} + x^{39} + x^{40} + x^{48} + x^{49} + x^{50} + x^{51} + x^{52}, \\ P_{\mathrm{R}}(x) &= \frac{1}{20}(1 + x^7 + x^9 + x^{11})\sum_{i=0}^{16} x^{5i}. \end{aligned}$$

Application of cosine apodization to the receive aperture results in a smoother combined T/R effective aperture function as shown in Fig. 9.

VIII. Sparse Array Design by Triangular Interpolation

Three different techniques can be used for such a design.

A. Design Method 1

Here we use the design method for linearly tapered effective aperture function with $r = s$, so that:

$$P_r(x) = \frac{1}{r}\sum_{i=0}^{r-1} x^i = \frac{1}{r}P_s(x). \tag{27}$$

As in the case of a linearly tapered effective aperture function, r must be a non-prime number so that $P_s(x)$ can be factorized. Fig. 10 shows an example of such a design with $r = s = 18$ and the following choices for transmit and receive polynomials.

$$\begin{aligned} P_{\mathrm{T}}(x) &= (1 + x)(1 + x + x^2)(1 + x^2 + x^4) \\ &= 1 + 2x + 3x^2 + 3x^3 + 3x^4 + 3x^5 + 2x^6 + x^7, \\ P_{\mathrm{R}}(x) &= \frac{1}{18}(1 + x^3 + x^6)(1 + x^6 + x^{12})(1 + x^9) \\ &= \frac{1}{18}(1 + x^3 + 2x^6 + 2x^9 + 3x^{12} + 3x^{15} \\ &\quad + 2x^{18} + 2x^{21} + x^{24} + x^{27}). \end{aligned}$$

B. Design Method 2

In this case, two triangularly weighted arrays $P_{\mathrm{T}}(x)$ and $P_{\mathrm{R}}(x)$ can be chosen such that missing elements in $P_{\mathrm{R}}(x)$ can be filled by those in $P_{\mathrm{T}}(x)$ [4].

Let $P_r(x) = \sum_{i=0}^{r-1} x^i$ with r being an odd integer. Let $m = (r - 1)/2$ and $P_s(x) = \sum_{i=0}^{s-1} x^{(m+1)i}$, where s is also an odd integer. Here, $P_{\mathrm{T}}(x)$ is obtained by triangularly weighting $P_r(x)$, and $P_{\mathrm{R}}(x)$ is obtained similarly from $P_s(x)$. A representative triangular weighting function for $P_{\mathrm{T}}(x)$ is noted here:

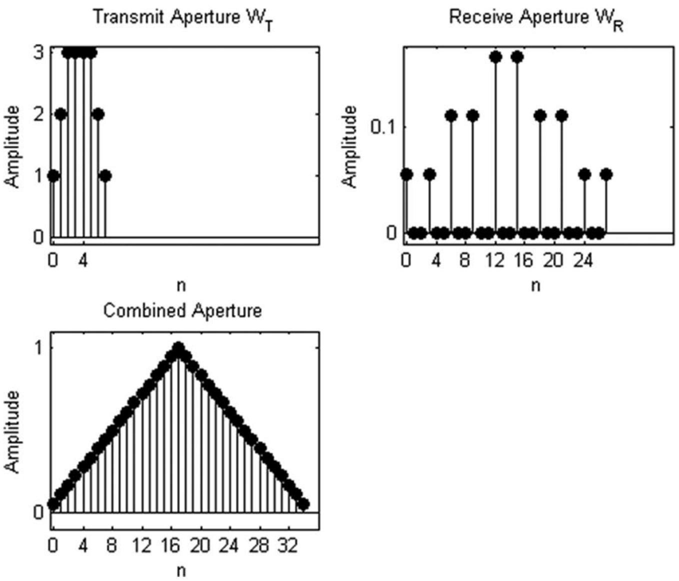

Fig. 10. Triangular array design for $r = s = 18$.

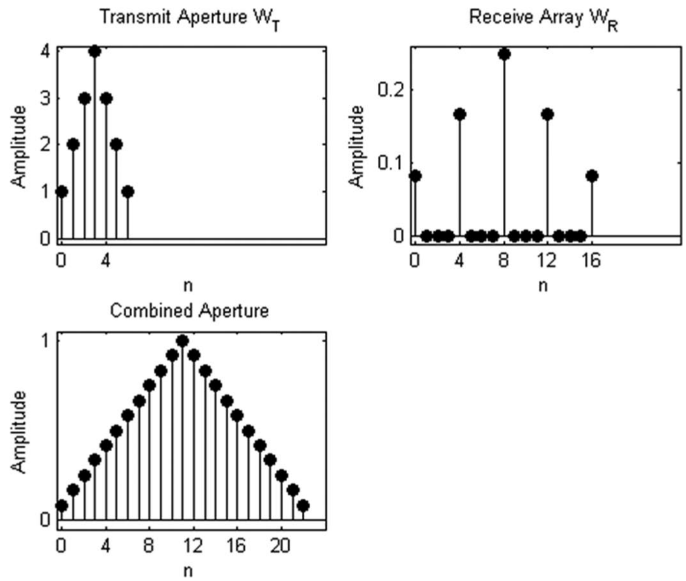

Fig. 11. Transmit, receive, and combined T/R arrays for triangular effective aperture function of Example 7.

$$w(i) = \begin{cases} i+1, & \text{for } 0 \le i \le m, \\ 2m - i + 1, & \text{for } m \le i \le 2m. \end{cases} \tag{28}$$

Thus, $P_{\mathrm{T}}(x)$ will have r consecutive elements (no missing elements) and $P_{\mathrm{R}}(x)$ will have m missing elements between each pair of nonzero elements.

A scaling factor, $4/(r + 1)(N_R + 1)$ can optionally be used with $P_{\mathrm{R}}(x)$ to make sure that the maximum magnitude of the combined T/R effective aperture function is unity. Here N_{R} represents the number of nonzero elements in the receive array.

Note that for a given choice of an odd integer r, there are multiple choices of the odd integer s as noted here:

$$(r+1)+1,\ 2(r+1)+1,\ 3(r+1)+1,\ \cdots$$

Using proper choices of s and r, the polynomials $P_r(x)$ and $P_s(x)$ can be determined. These polynomials lead to $P_{\mathrm{T}}(x)$ and $P_{\mathrm{R}}(x)$ after applying proper weighting functions as described.

Example 7: Consider $r = 7$, $s = 17$. Thus,

$$P_r(x) = 1 + x + x^2 + x^3 + x^4 + x^5 + x^6,$$
$$P_s(x) = 1 + x^4 + x^8 + x^{12} + x^{16}.$$

The triangular transmit and receive arrays can be represented as

$$P_{\mathrm{T}}(x) = 1 + 2x + 3x^2 + 4x^3 + 3x^4 + 2x^5 + x^6,$$
$$P_{\mathrm{R}}(x) = (1 + 2x^4 + 3x^8 + 2x^{12} + x^{16})/12.$$

Note that the total number of elements in the two arrays is 12. The SF achieved in this design is $23/12 = 1.91$. The designed arrays are shown in Fig. 11.

The SR obtained from this design is included in Table I.

C. Design Method 3

In this case, a transmit array $P_{\mathrm{T}}(x)$ can be formed by starting with a triangular weighted array $P_r(x)$ with an odd number r of elements

$$P_r(x) = \sum_{i=0}^{r-1} w(i)x^i, \tag{29}$$

where $w(i)$ is as defined in (28).

The transmit array is obtained by replicating the $P_r(x)$ array at intervals of

$$k = (m+2)(m+1). \tag{30}$$

Thus,

$$P_{\mathrm{T}}(x) = P_r(x)\sum_{i=0}^{t} x^{ki}. \tag{31}$$

The receive array $P_{\mathrm{R}}(x)$ will have a triangular rise followed by a flat region, followed by a triangular fall. Each pair of nonzero elements in $P_{\mathrm{R}}(x)$ will be separated by $m + 1$ zero elements.

$$P_{\mathrm{R}}(x) = \left[\sum_{i=0}^{m}(i+1)x^{(m+1)i} + \sum_{i=m+1}^{n}(m+2)x^{(m+1)i} + \sum_{i=n+1}^{m+n+1}(m+2-i+n)x^{(m+1)i}\right]/\text{scale factor},$$
$$n = (m+2)t + m + 1, \tag{32}$$

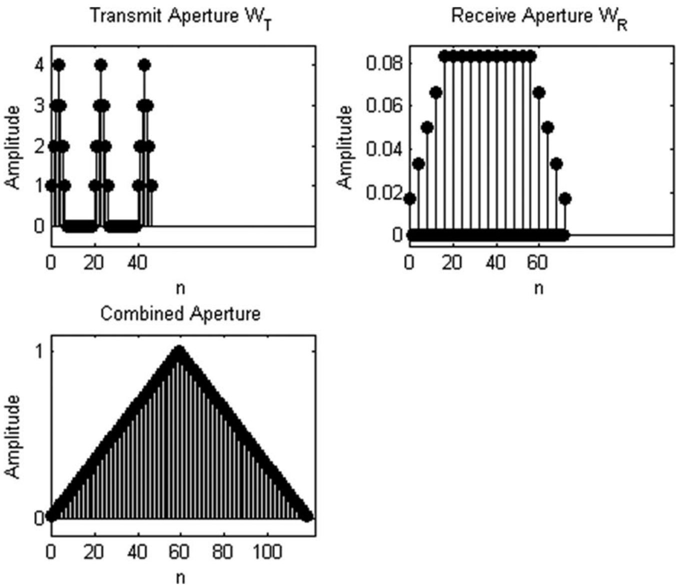

Fig. 12. Transmit, receive, and combined T/R arrays for triangular effective aperture function in Example 8.

and a properly chosen scale factor normalizes the amplitude of the combined T/R effective aperture function.

By design, the receive array will have element spacing of $\lambda/2$ and transmit array elements will not have fixed spacing. The following example clarifies the design.

Example 8: Let $r = 7$, $m = (r - 1)/2 = 3$ and $t = 2$. In this case, $P_r(x) = 1 + 2x + 3x^2 + 4x^3 + 3x^4 + 2x^5 + x^6$ and $k = (3 + 2) \times (3 + 1) = 20$. From (31), the transmit array is given by

$$P_{\mathrm{T}}(x) = P_r(x)(1 + x^{20} + x^{40}).$$

The receive array obtained from (32) is found to be

$$P_{\mathrm{R}}(x) = \left(1 + 2x^4 + 3x^8 + 4x^{12} + 5x^{16}\sum_{i=0}^{10} x^{4i} + 4x^{60} + 3x^{64} + 2x^{68} + x^{72}\right)/60.$$

The designed array patterns are plotted in Fig. 12. The total number of elements of the fully populated combined T/R effective aperture function is 119. However, the sum of nonzero elements in transmit and receive arrays is only $21 + 19 = 40$. Thus, this design is sparse with an SF of 2.975.

It can be noted from all of the plots for triangular effective aperture function spectra that the MW becomes narrower as more nonzero elements are added to the function. However, the relative sidelobe rejection increases slightly by increasing the number of elements in the aperture function.

IX. Sparse Array Design by Vernier Interpolation

Vernier interpolation between receive and transmit sparse arrays leads to a combined T/R effective aperture function that has equal spacing, exhibits an irregular shape, and has a few elements missing at each end of the aperture. The irregularity in shape can be smoothed out by applying an apodization function such as cosine^2. In the following, we describe the design method of such sparse arrays and illustrate with two examples.

In general, vernier interpolation involves choosing a polynomial $P_{\mathrm{R}}(x)$ with elements separated by $p - 1$ zero elements and $P_{\mathrm{T}}(x)$ with elements separated by p zero elements. Let

$$P_{\mathrm{R}}(x) = \sum_{i=0}^{r-1} x^{(p-1)i} \tag{33}$$

and

$$P_{\mathrm{T}}(x) = \sum_{i=0}^{s-1} x^{pi}, \tag{34}$$

where $p > 1$ is an integer.

It should be noted that for $p = 2$, no elements will be missing from the combined T/R effective aperture function. In general, the number of missing elements from the combined T/R effective aperture function is given by $(p - 1)(p - 2)$.

A. Case 1

In Case 1, the orders of the polynomials $P_{\mathrm{R}}(x)$ and $P_{\mathrm{T}}(x)$ are equal. In this case, r and s must satisfy

$$(r-1)(p-1) = (s-1)p = k. \tag{35}$$

In order for the equality in (35) to hold, k must be divisible both by p and $p - 1$. Therefore, k is of the form

$$k = np(p-1), \quad n = 1, 2, 3, \ldots. \tag{36}$$

For example, if we choose $p = 3$, then $k = 6, 12, 18, 24, \ldots$, etc.

Example 9: Let $p = 3$, and $k = 42$. This will result in a combined T/R effective aperture function with 83 nonzero elements. Here we choose $P_{\mathrm{R}}(x) = \sum_{i=0}^{21} x^{2i}$ and $P_{\mathrm{T}}(x) = \sum_{i=0}^{14} x^{3i}$. The combined T/R effective aperture function realized is shown in Fig. 13 and has 85 ($= 2k + 1$) elements. It is not smooth and exhibits ragged edges.

Application of cosine apodization smoothes out the combined T/R effective aperture function considerably, as shown in Fig. 14, and helps enhance the relative sidelobe rejection as shown in Table I.

B. Case 2

Case 2 places no restrictions on the order of the transmit and receive polynomials. In this case, the total number of elements in the designed array (including zero elements) will be given by $p(s - 1) + (p - 1)(r - 1) + 1$. The total

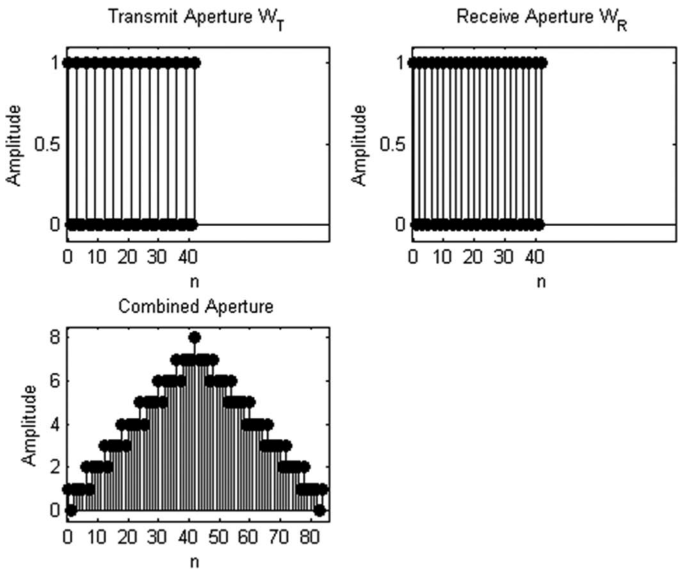

Fig. 13. Transmit, receive, and combined T/R effective aperture functions for Example 9 (without apodization).

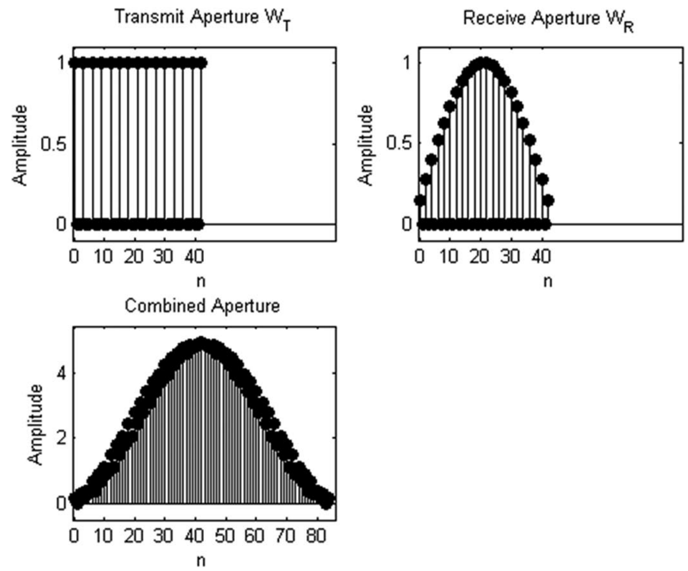

Fig. 14. Transmit, receive (with cosine apodization), and combined T/R effective aperture function in Example 9.

number of nonzero elements of the designed transmit and receive arrays will be $r + s$. Multiple designs are possible, given the specification of the total number of nonzero elements of an array and the value of p.

Example 10: Let us consider the design example of a 128-element full array from [4] with $p = 4$. Note that the choice of $p = 4$ results in 6 zero elements in the combined aperture. Here we need to solve $4(s - 1) + 3(r - 1) = 127$. There are multiple solutions for the two unknowns that will result in different numbers of nonzero elements forming the combined T/R effective aperture function.

For $s = 23$ and $r = 14$, the radiation pattern of the overall array exhibits an SR of -19.8 dB with a MW of 0.017578. On the other hand, for $s = 17$ and $r = 22$, the radiation pattern of the designed 39-element array is found to be -26.4 dB with the same MW as before. Fig. 15 shows the designed arrays.

X. Comparison of Sparse Array Designs

In the following, we define various performance parameters used in this paper.

A. Sparsity Factor (SF)

SF is a measure of sparseness of the design and is defined as the ratio $N_{\text{eff}}/(N_{\text{T}} + N_{\text{R}})$, where N_{eff}, N_{T}, and N_{R} are the numbers of nonzero elements in the combined aperture, transmit aperture, and receive aperture, respectively. This ratio should preferably be larger than 1 for a sparse array design. This definition of sparsity factor assumes the same complexity of implementation of the transmit and receive arrays. In practice, the receive aperture requires dynamic apodization and focusing capabilities, whereas the transmit aperture requires high-power drive circuits.

B. Sidelobe Rejection (SR)

The SR measure is the difference in the gain level in decibels between the height of the mainlobe and that of the highest sidelobe peak of the combined T/R effective radiation pattern. The larger the value of this parameter is, the better the selectivity of the antenna or transducer array will be. Note that SR is not very important in medical ultrasound imaging because the object being imaged is a continuous speckle source of varying amplitude. The leakage factor is more informative for medical ultrasound.

C. Mainlobe Width (MW)

The MW is measured as the difference in angular position (in radians) between the 3-dB points of the mainlobe of the combined T/R effective radiation pattern. A smaller value indicates smaller angular extent and better selectivity.

D. Leakage Factor (LF)

The LF is measured as a ratio of power in the sidelobes to the total window power.

E. Element Reduction Factor (ERF)

The ERF is a measure of the sparseness of the staircase-like combined T/R effective aperture function design, defined as the ratio $(N_r + N_s)/(N_{\text{T}} + N_{\text{R}})$, where N_r, N_s, N_{T}, and N_{R} denote the number of nonzero elements of polynomials $P_r(x)$, $P_s(x)$, $P_{\text{T}}(x)$, and $P_{\text{R}}(x)$, respectively. Normally, the SF will be greater than or equal to the

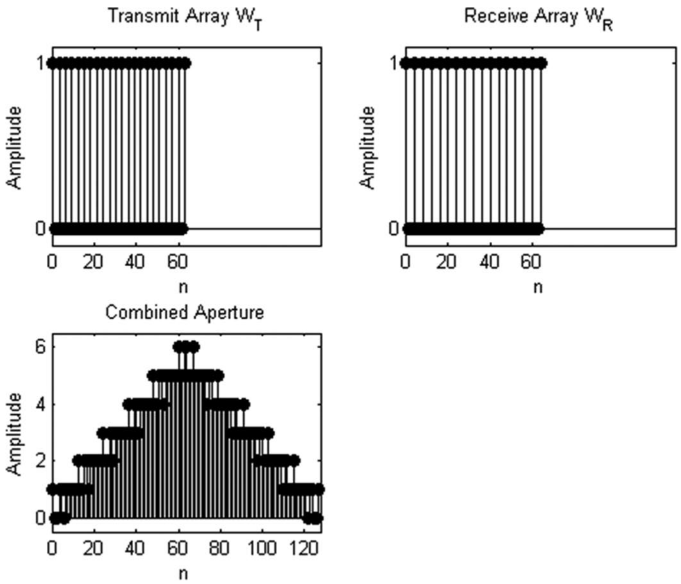

Fig. 15. Transmit, receive, and combined T/R effective aperture functions for Example 10.

ERF. The ERF is an excellent measure often used in designing ultrasound scanners [8].

F. SNR Loss

A measure of SNR difference between combined T/R effective aperture function and the corresponding uniform fully populated array measured as the difference in beamforming gain [23] in decibels. The beamforming gains for both the designed and fully populated arrays are determined at the peak of the mainlobe at 0 rad.

G. Composite SNR Loss

This performance parameter is especially important for high-sensitivity applications such as color flow imaging. It is computed by adding the SNR loss corresponding to each designed array (transmit and receive, respectively) with respect to their full-array counterparts. The composite SNR loss is obtained as $20\log_{10}(N_{\mathrm{TF}}/N_{\mathrm{T}}) + 10\log_{10}(N_{\mathrm{RF}}/N_{\mathrm{R}})$ in decibels, where N_{TF} and N_{RF}, respectively, represent the element counts of equivalent full transmit and receive arrays. In this definition, we assumed constant voltage drive on transmit and constant gain and noise factor on receive array.

Based upon these figures of merit, Table I summarizes the results from the design examples in this paper.

The design methods described in this paper are simple to implement and result in different performances of the combined T/R effective aperture functions. As seen from Table I, linearly tapered and mixed tapered staircase effective aperture functions exhibit very low leakage factors. MW is also quite low for mixed tapered staircase effective aperture function. On the other hand, vernier interpolation leads to high sparsity and high ERF designs which are highly desirable when 1-D arrays are used to develop separable 2-D arrays. SNR loss is lowest for staircase effective aperture functions. However, SNR loss for linearly tapered, mixed tapered staircase, triangular, and vernier effective aperture functions are comparable if no apodization is applied. Adding cosine apodization results in higher SNR loss in every case.

On the other hand, composite SNR loss factor shows a different set of behavior among various designs. Triangular and vernier effective aperture functions exhibit fairly high composite SNR losses when we assume constant voltage drive on transmit and constant gain and noise factor on receive array. Different variations of staircase effective aperture functions exhibit comparable composite SNR loss factors. The linearly tapered effective aperture function of Example 3 exhibits low composite SNR loss. Thus a high ERF may not always be desirable (as seen for the case of vernier interpolation), especially when low composite SNR loss is a major system requirement, as in color flow imaging.

In Table II we list results from linearly tapered, staircase, and mixed tapered staircase aperture functions, and vernier interpolation with a fixed number of elements. We hold N_{eff} constant at 85 among the various designs shown in the table. The results in this table allow us to compare various design techniques for the same size of the combined T/R aperture function.

Here are some notes on the results in Table II.

1) Linearly tapered effective aperture function SR increases as r increases. Mixed tapered staircase aperture functions also show similar behavior.
2) Linearly tapered effective aperture function MW decreases as r decreases.
3) Staircase effective aperture functions exhibit more complex dependence on the various parameters. However, SR seems to have a parabolic relationship with increasing r (and decreasing s) with optimum in the middle.
4) Mixed tapered staircase effective aperture functions exhibit properties similar to those noted in the previous point.
5) SNR losses continue to increase as the design progresses from linearly tapered through mixed tapered staircase effective aperture functions even for the same number of full array elements. Vernier interpolation results in SNR losses comparable to some mixed tapered staircase arrays.
6) Composite SNR loss does not seem to follow a set pattern of increase or decrease. In general, staircase and vernier effective aperture functions exhibit larger composite SNR losses compared with the other types of effective aperture functions.
7) None of the designs included in the table need weighting of transmit or receive arrays. In some cases, we have applied scale factors on receive arrays to make combined T/R array elements normalized to unity. Such scaling does not affect the performance mea-

TABLE II. Comparison of Sparse Array Designs With Fixed 85 Elements.

Type	r	N_T	N_R	ERF	Leakage factor (%)	Sidelobe rejection (dB)	Mainlobe width (rad)	SNR loss (dB)	Composite SNR loss (dB)
Linearly tapered	2	12	14	3.308	8.82	−13.3	0.0195	0.0255	7.231
Linearly tapered	5	27	15	2.048	7.71	−13.4	0.0215	0.1227	5.9476
Linearly tapered	11	15	55	1.229	5.64	−13.9	0.0215	0.3277	1.109
Linearly tapered	22	32	44	1.132	2.22	−16.8	0.0254	0.705	0.8894
Staircase	21	25	13	1.842	2.09	−17.7	0.0254	0.5947	6.7139
Staircase	31	15	11	2.231	2.2	−21	0.0254	0.6848	14.0213
Staircase	31	35	11	1.348	0.51	−26.9	0.0273	0.879	6.6618
Staircase	31	30	11	1.488	0.59	−27.8	0.0273	0.8552	8.0007
Staircase	35	9	17	2.077	3.08	−20.8	0.0254	0.6924	16.8767
Staircase	41	9	25	1.471	1.48	−22.8	0.0254	0.8539	15.7236
Staircase	41	9	30	1.308	1.09	−24.8	0.0273	0.92	14.9317
Mixed tapered staircase $(1 + x^6)$	31	20	22	1.5	0.62	−24.8	0.0273	0.9461	7.3619
Mixed tapered staircase $(1 + x^5 + x^6)$	31	15	44	1.136	0.55	−24.7	0.0273	0.9542	2.3161
Mixed tapered staircase $(1 + x^6)$	35	15	19	1.794	0.44	−30.4	0.0273	1.0756	10.9215
Mixed tapered staircase $(1 + x^4)$	35	18	34	1.211	0.26	−31.2	0.0273	1.0534	7.1928
Mixed tapered staircase $(1 + x^5)$	36	30	20	1.24	0.33	−32.4	0.0273	1.1031	5.9895
Mixed tapered staircase $(1 + x^3 + x^5)$	36	20	30	1.36	0.19	−32	0.0273	1.1084	7.7505
Mixed tapered staircase $(1 + x^5)$	41	18	30	1.1875	0.45	−27.2	0.0273	1.1397	9.0228
Vernier interpolation $(p = 4)$	49	10	17	3.1481	3.35	−28.9	0.0273	1.0601	15.9615

sures (namely LF, MW, SR, and SNR loss) of the designed arrays.

Progressively better SR result is obtained as we move from linearly tapered to staircase to mixed tapered staircase effective aperture functions.

Vernier interpolation shows excellent MW and good SR. However, the leakage factor is high, indicating that there is quite a bit of energy in the sidelobes. The combined T/R effective aperture function has 6 zero elements. Still, the ERF of the design is quite high, indicating it to be quite sparse. In this comparison, we did not include triangular interpolation for the following reason. Triangular interpolation leads to a triangular-shaped combined T/R effective aperture function which is not considered to be a very desirable function without apodization.

Note that none of the design techniques (including vernier, which applies no apodization) described in this paper require any weighting of the transmit or receive aperture functions except to normalize the maximum weight factors for combined T/R aperture function to unity. When cosine apodization is applied, the receive array weight factors are no longer unity, resulting in additional hardware complexity.

In this paper, the model of the designed arrays assumes far-field operation of a continuous wave source. This is rarely the case for ultrasound imaging. Clinical systems operate in the near field at low f/numbers. Focusing of both transmit and receive apertures is required. The bandwidth is typically 60 to 70% and often approaches 100%. Near-field operation can remove the simple Fourier transform (FT) relation between the aperture function and the radiation pattern, or at least require a complex aperture function including the focusing term. Broadband operation diffuses sidelobes, minimizing interference effects far from the mainlobe. Many details in sidelobe structure are diffused with broadband operation; subtle differences between aperture functions often result in non-negligible differences to broadband sidelobe patterns.

Because ultrasound imaging systems operate primarily in the aperture's near field, focusing effects dominate the radiation patterns. In modern scanners, dynamic focusing and apodization is performed on receive so that the receive beam pattern can be reasonably modeled as the FT of the instantaneous aperture. This is not the case for the transmitter. The transmitter is focused to a fixed depth, which means most of the imaging volume is not at the focal plane of the transmitter. The asymmetry between transmit and receive functions in a real-time scanner is a major feature of ultrasound imaging that must be addressed in any practical design. Note that in this paper, we have applied apodization on the receive array only.

Harmonic imaging and other non-linear imaging methods are now the default conditions for many clinical applications. For example, in echocardiography nearly all clinical scans are performed using some form of harmonic imaging. Any practical sparse array design must be evaluated for both fundamental mode and harmonic imaging;

because transmit and receive arrays operate over different frequency ranges for non-linear imaging, a sparse array designed for fundamental imaging may not work well for nonlinear imaging. Further studies are needed to understand the efficiency of the designed sparse arrays in nonlinear imaging.

XI. Conclusion

In this paper, we have presented several simple and elegant methods for the design of sparse arrays. The mathematical foundation of design of sparse arrays for uniform, linearly tapered, staircase, and mixed tapered staircase combined effective T/R aperture functions is based on a polynomial factorization theorem. This theorem is included herein and its application in designs is illustrated using several examples. Additional heuristic design techniques based upon triangular and vernier interpolations are also explained using appropriate polynomial choices.

Acknowledgments

The authors are indebted to the anonymous reviewers for their constructive comments, which significantly improved this paper.

References

[1] B. D. Steinberg, *Principles of Aperture and Array Systems Design.* New York, NY: Wiley, 1976.
[2] D. H. Johnson and D. E. Dudgeon, *Array Signal Processing: Concept and Techniques.* Englewood Cliffs, NJ: Prentice-Hall, 1993.
[3] P. S. Naidu, *Sensor Array Signal Processing.* 2nd ed., Boca Raton, FL: CRC Press, 2009.
[4] G. Lockwood, P. Li, M. O'Donnell, and F. Foster, "Optimizing the radiation pattern of sparse periodic linear arrays," *IEEE Trans. Ultrason. Ferroelectr. Freq. Control*, vol. 43, no. 1, pp. 7–14, Jan. 1996.
[5] B. D. Steinberg, "The peak sidelobe of the phased array having randomly located elements," *IEEE Trans. Antenn. Propag.*, vol. 20, no. 2, pp. 129–136, Mar. 1972.
[6] R. M. Leahy and B. D. Jeffs, "On the design of maximally sparse beamforming arrays," *IEEE Trans. Antenn. Propag.*, vol. 39, no. 8, pp. 1178–1187, Aug. 1991.
[7] S. Holm, B. Elgetun, and G. Dahl, "Properties of the beampattern of weight- and layout-optimized sparse arrays," *IEEE Trans. Ultrason. Ferroelectr. Freq. Control*, vol. 44, no. 5, pp. 983–991, Sep. 1997.
[8] R. L. Haupt, "Thinned arrays using genetic algorithms," *IEEE Trans. Antenn. Propag.*, vol. 42, no. 7, pp. 993–999, Jul. 1994.
[9] D. S. Weile and E. Michielssen, "Integer-coded Pareto genetic algorithm design of antenna arrays," *Electron. Lett.*, vol. 32, no. 9, pp. 1744–1745, 1996.
[10] A. Austeng, S. Holm, P. K. Weber, N. Aakvaag, and K. Iranpour, "1D and 2D algorithmically optimized sparse arrays," *Proc. 1997 IEEE Ultrasonics Symp.*, 1997, pp. 1683–1686.
[11] A. Lommi, A. Massa, E. Storti, and A. Trucco, "Side lobe reduction in sparse linear arrays by genetic algorithms," *Microw. Opt. Technol. Lett.*, vol. 32, no. 3, pp. 194–196, Feb. 5, 2002.
[12] S. Caorsi, A. Lommi, A. Massa, S. Piffer, and A. Trucco, "Planar antenna array design with a multi-purpose GA-based procedure," *Microw. Opt. Technol. Lett.*, vol. 35, no. 6, pp. 428–430, Dec. 20, 2002.
[13] A. Massa, M. Donelli, F. De Natale, S. Caorsi, and A. Lommi, "Planar antenna array control with genetic algorithms and adaptive array theory," *IEEE Trans. Antenn. Propag.*, vol. 52, no. 11, pp. 2919–2924, Nov. 2004.
[14] A. Trucco and V. Murino, "Stochastic optimization of linear sparse arrays," *IEEE J. Oceanic Eng.*, vol. 24, no. 3, pp. 291–299, Jul. 1999.
[15] A. Trucco, "Thinning and weighting of large planar arrays by simulated annealing," *IEEE Trans. Ultrason. Ferroelectr. Freq. Control*, vol. 46, no. 2, pp. 347–355, Mar. 1999.
[16] A. Austeng and S. Holm, "Sparse 2-D arrays for 3-D phased array imaging—Design methods," *IEEE Trans. Ultrason. Ferroelectr. Freq. Control*, vol. 49, no. 8, pp. 1073–1086, Aug. 2002.
[17] M. Donelli, A. Martini, and A. Massa, "A hybrid approach based on PSO and Hadamard difference sets for the synthesis of square thinned arrays," *IEEE Trans. Antenn. Propag.*, vol. 57, no. 8, pp. 2491–2495, Aug. 2009.
[18] S. K. Mitra, *Digital Signal Processing: A Computer-Based Approach,* 3rd ed., New York, NY: McGraw-Hill, 2006.
[19] S. K. Mitra, M. K. Tchobanou, and M. I. Bryukhanov, "A general method for designing sparse antenna arrays," *Proc.* 17th *European Conf. Circuit Theory and Design,* Cork, Ireland, Aug. 2005, vol. II, pp. 263–266.
[20] S. K. Mitra, M. K. Tchobanou, and G. Jovanovic-Dolecek, "A simple approach to the design of one-dimensional sparse antenna arrays," *Proc. IEEE Int. Symp. Circuits & Systems,* Vancouver, B.C., Canada, May 2004, vol. III, pp. 541–544.
[21] S. K. Mitra, G. Jovanovic-Dolecek, and M. K. Tchobanou, "On the design of one-dimensional sparse arrays with apodized end elements," *Proc. European Signal Processing Conf.,* Vienna, Austria, Sep. 2004, pp. 2239–2241.
[22] K. Mondal and S. K. Mitra, "Design of sparse arrays with high sidelobe rejection," *Proc. IEEE Asia Pacific Conf. Circuits and Systems*, Macau, China, Dec. 2008, pp. 980–983.
[23] D. G. Manolakis, V. K. Ingle, and S. M. Kogon, *Statistical and Adaptive Signal Processing.* New York, NY: McGraw-Hill, 2000.

Sanjit K. Mitra obtained his B.Sc. degree with honors in physics (1953) and the M.Sc. (Tech.) degree in radio physics and electronics (1956) in India. He then obtained his M.S. (1960) and Ph.D. (1962) degrees in electrical engineering from U.C. Berkeley. He is the Stephen and Etta Varra Professor of Engineering in the Ming Hsieh Department of Electrical Engineering, University of Southern California, Los Angeles. He has published more than 660 papers in the areas of analog and digital signal processing, and image processing. He has also authored or co-authored twelve books, and holds five patents. Dr. Mitra has served IEEE in various capacities including service as the President of the IEEE Circuits & Systems Society in 1986, and has held visiting appointments in Australia, Austria, Brazil, Croatia, Finland, Germany, India, Japan, Norway, Singapore, Turkey, and the United Kingdom.

Dr. Mitra is the recipient of the 1973 F.E. Terman Award and the 1985 AT&T Foundation Award of the American Society of Engineering Education; the 1989 Education Award and the 2000 Mac Van Valkenburg Society Award of the IEEE Circuits & Systems Society; the Distinguished Senior U.S. Scientist Award from the Alexander von Humboldt Foundation of Germany in 1989; the 1996 Technical Achievement Award, the 2001 Society Award, and the 2006 Education Award of the IEEE Signal Processing Society; the IEEE Millennium Medal in 2000; the McGraw-Hill/Jacob Millman Award of the IEEE Education Society in 2001; the 2002 Technical Achievement Award and the 2009 Athanasios Papoulis Award of the European Association for Signal Processing (EURASIP); the 2005 SPIE Technology Achievement Award of the International Society for Optical Engineers; the University Medal of the Slovak Technical University, Bratislava, Slovakia in 2005; and the 2006 IEEE James H. Mulligan, Jr. Education Medal. He is the co-recipient of the 2000 Blumlein-Browne-Willans Premium of the Institution of Electrical Engineers (London) and the 2001 IEEE Transactions on Circuits & Systems for Video Technology Best Paper Award. He has been awarded Honorary Doctorate degrees from the Tampere University of Technology, Finland, the Technical University of Bucharest, Romania, and the Technical University of Iasi, Romania. He is a member of the U.S.

National Academy of Engineering, a member of the Norwegian Academy of Technological Sciences, an Academician of the Academy of Finland, a corresponding member of the Croatian Academy of Sciences and Arts, a corresponding member of the Academy of Engineering, Mexico, and a Foreign Fellow of the National Academy of Sciences, India, and the Indian National Academy of Engineering. Dr. Mitra is a Fellow of the IEEE, AAAS, and SPIE, and a member of EURASIP.

Kalyan Mondal (M'80–SM'91) received the B. Sc. degree with honors in physics in 1969, the B. Tech. and M.Tech. degrees in radiophysics and electronics in 1972 and 1974, respectively, from the University of Calcutta, India, and the Ph.D. degree in electrical engineering from the University of California, Santa Barbara, in 1978.

From 1978 to 1979, he was a Lecturer and Postgraduate Researcher at the Department of Electrical and Computer Engineering, University of California, Santa Barbara. He was an Assistant Professor at the Department of Electrical Engineering, Lehigh University, Bethlehem, PA, between 1980 and 1983. In January 1982, he joined the AT&T Bell Laboratories as a Member of the Technical Staff and was promoted to the positions of Distinguished Member of Technical Staff in 1987 and Technical Manager in 1996. He was a member of the design team that developed the first 32-bit floating-point digital signal processor and a co-winner of the 1985 IEEE International Solid State Circuits Conference Outstanding Paper Presentation Award. He was involved with the development of industry's first MPEG-2 simple profile video decoder IC at Bell Laboratories, Murray Hill, NJ. While at Lucent Technologies, he led the development of cable modem receiver, ATSC terrestrial broadcast baseband receiver, and Sonet add drop multiplexer VLSIs. Later he was involved in managing the development of RapidIO and Firewire high speed interface ICs at Agere Systems, Allentown, PA. He joined Fairleigh Dickinson University at Teaneck, NJ in 2006 as an Assistant Professor of Electrical Engineering and Coordinator of Information Technology program and was promoted to the rank of Associate Professor in 2010. He has been a Consultant to the LSI Corp., Allentown, PA. He holds eight patents.

Dr. Mondal is a life member of Eta Kappa Nu. He was the Founding Chairperson of the Lehigh Valley Chapter of the IEEE Circuits and Systems Society in 1987 to 1988. He was a member of the Technical Program Committee of the 1988 IEEE International Symposium on Circuits and Systems held in Finland. He also has served IEEE Circuits and Systems Society ADCOM as an elected member during 1989 to 1992.

Mikhail K. Tchobanou was born in 1960 in the Moscow region, Russia. He graduated in 1983 from the Moscow Power Engineering Institute (MPEI) and received the Ph.D. and Doctor of Science degrees in multi-dimensional signal processing in 1987 and 2008, respectively. He was an Associate Professor at MPEI, and became a Professor in 2010.

His fields of interest include wavelet transform; approximation methods; and application of computational algebra in signal processing and in sparse antenna array design, multi-dimensional filter bank design, compression and de-noising, and interpolation of multi-dimensional signals.

From 2008 through 2010, he worked in the Samsung Research Center. He presently is a Vice-head of Division in the General Radio-Frequency Center in Moscow, Russia. He worked as a Visiting researcher in Norway (1999), the United States (from 2000 to 2003), Japan (in 2004, 2006, and 2008), and Finland (2006).

He is an Associate Editor of the international journal *Multidimensional Systems and Signal Processing*. He is an IEEE member, was Co-Chair of Organizing Committee of 7th International Workshop on Spectral Methods and Multirate Signal Processing SMMSP-2007 (September 1–2, 2007) in Moscow, Russia [jointly organized with Tampere International Centre of Signal Processing (TICSP), Finland], member of the Organizing Committees of the international conference on Digital Signal Processing and its Applications (DSPA) and the International Conference of Informatization Academy (Russia). His three M.Sc. students received the Medal of the Russian Academy of Sciences in year 2004 for the best work written by students in Russia in the field of Informatics, Computer Science, and Communication.

Gordana Jovanovic Dolecek received a B.S. degree from the Department of Electrical Engineering, University of Sarajevo, an M.Sc. degree from University of Belgrade, and a Ph.D. degree from the Faculty of Electrical Engineering, University of Sarajevo. She was professor at the Faculty of Electrical Engineering, University of Sarajevo until 1993, and from 1993 to 1995, she was with the Institute Mihailo Pupin, Belgrade. In 1995, she joined Institute INAOE, Department for Electronics, Puebla, Mexico, where she works as a full professor. During 2001 to 2002 and 2006 she was with Department of Electrical & Computer Engineering, University of California, Santa Barbara, as visiting researcher. She was with San Diego State University as visiting researcher on a sabbatical leave in 2008 to 2009. She is the author of three books, editor of one book, and author of more than 200 papers. Her research interests include digital signal processing and digital communications. She is a Senior Member of IEEE, a member of Mexican Academy of Science, and a member of National Researcher System (SNI) Mexico.